Full paper

Applied Organometallic Chemistry

Received: 21 May 2016 Revised: 7 June 2016 Accepted: 9 June 2016 Published online in Wiley Online Library

(wileyonlinelibrary.com) DOI 10.1002/aoc.3555

Ni(II) and Cu(II) complexes with ONNO asymmetric tetradentate Schiff base ligand: synthesis, spectroscopic characterization, theoretical calculations, DNA interaction and antimicrobial studies

Laila H. Abdel-Rahman[a], Ahmed M. Abu-Dief[a]*, H. Moustafa[b] and Samar Kamel Hamdan[a]

A novel Schiff base, namely *Z*-3-((2-((*E*)-(2-hydroxynaphthyl)methylene)amino)-5-nitrophenylimino)-1,3-dihydroindin-2-one, was synthesized from the condensation of 2-hydroxy-1-naphthaldehyde and isatin with 4-nitro-*o*-phenylenediamine. It was structurally characterized on the basis of ^{1}H NMR, ^{13}C NMR and infrared spectra and elemental analyses. In addition, Ni(II) and Cu(II) complexes of the Schiff base ligand were prepared. The nature of bonding and the stereochemistry of the investigated complexes were elucidated using several techniques, including elemental analysis (C, H, N), Fourier transform infrared and electronic spectroscopies and molar conductivity. The thermal behaviours of the complexes were studied and kinetic–thermodynamic parameters were determined using the Coats–Redfern method. Density functional theory calculations at the B3LYP/6-311G++ (d, p) level of theory were carried out to explain the equilibrium geometry of the ligand. The optimized geometry parameters of the complexes were evaluated using LANL2DZ basis set. The total energy of highest occupied and lowest unoccupied molecular orbitals, Mullikan atomic charges, dipole moment and orientation are discussed. Moreover, the interaction of the metal complexes with calf thymus DNA (CT-DNA) was explored using electronic spectra, viscosity measurements and gel electrophoresis. The experimental evidence indicated that the two complexes could strongly bind to CT-DNA via an intercalation mechanism. The intrinsic binding constants of the investigated Ni(II) and Cu(II) complexes with CT-DNA were 1.02×10^{6} and 2.15×10^{6} M^{-1}, respectively, which are higher than that of the standard ethidium bromide. Furthermore, the bio-efficacy of the ligand and its complexes was examined *in vitro* against the growth of bacteria and fungi to evaluate the antimicrobial potential. Based on the obtained results, the prepared complexes have promise for use as drugs. Copyright © 2016 John Wiley & Sons, Ltd.

Additional supporting information may be found in the online version of this article at the publisher's web site.

Keywords: asymmetric Schiff base ligand; DFT studies; TGA; DNA interaction; electrophoresis

Introduction

Schiff base ligands have played a key role in the development of coordination chemistry. Schiff base ligands with N_2O_2 donor atoms are well known to coordinate with a variety of metal ions. They have attracted much interest in recent years, due to their ease of synthesis, their stability under a variety of oxidative and reductive conditions and their structural versatility associated with various applications.[1–4] Schiff base complexes of transition metals have a wide range of applications due to their biocidal activity against bacteria, fungi and certain types of tumours.[5–8] These compounds are also utilized in magnetic and optoelectronic technologies for their large nonlinear responses.[9,10] The interest in the design, preparation and characterization of transition metal complexes of unsymmetric Schiff base ligands has arisen from the recognition that coordinated ligands around central metal ions in natural systems are unsymmetric.[11–13] As an important pharmacophore responsible for biological activity, isatin scaffold is an applicable lead structure for the synthesis of efficient chemotherapeutic agents.[14] Schiff base ligands derived from isatin exhibit many pharmacological effects like antimicrobial, antiviral, anticonvulsant, anticancer, antimalarial, herbicidal and anti-inflammatory activities.[15–17]

The literature reveals that Schiff base complexes of isatin and 4-nitro-*o*-phenylenediamine have not been much studied. Thus, we describe the preparation of Ni (II) and Cu(II) complexes with an asymmetric Schiff base ligand and the characterization of them using various techniques. Furthermore, we describe a comparative

* *Correspondence to: Ahmed M. Abu-Dief, Chemistry Department, Faculty of Science, Sohag University, 82534 Sohag, Egypt. E-mail: ahmed_benzoic@yahoo.com*

a *Chemistry Department, Faculty of Science, Faculty of Science, Sohag University, 82534, Sohag, Egypt*

b *Chemistry Department, Faculty of Science, Cairo University, 12613, Giza, Egypt*

study of DNA binding towards the prepared complexes and their various biological properties.

Experimental

Materials

All the starting materials of chemicals used in this investigation such as 2-hydroxy-1-naphthaldehyde, isatin, 4-nitro-*o*-phenylenediamine and the metal salts $Cu(CH_3COO)_2{\cdot}H_2O$ and $Ni(NO_3)_2{\cdot}6H_2O$, calf thymus DNA (CT-DNA) and Tris were purchased from Sigma-Aldrich Chemie (Germany). Spectroscopic grade ethanol, dimethylsulfoxide (DMSO), dimethylformamide (DMF) and HCl were used.

Instrumentation

NMR spectra were recorded with an FT-NMR spectrometer (Bruker ARX 400.1) at 400 MHz (^{1}H) and 100.6 MHz (^{13}C) in DMSO-d_6 at Central Lab, Chemistry Department, Faculty of Science, Sohag University. The ^{1}H and ^{13}C chemical shifts are presented in ppm. Coupling constants indicate J_{HH} in ^{1}H unless denoted otherwise. The melting point of the prepared Schiff base ligand and decomposition temperatures of its complexes were determined using a melting point apparatus (Gallenkamp, UK). The prepared Schiff base ligand and its complexes were subjected to (C, H, N) elemental analysis which was carried out with a PerkinElmer model 240c elemental analyser. The molar conductivity measurements of freshly prepared solutions of 1×10^{-3} and 4×10^{-4} mol cm^{-3} in DMF were measured using a Jenway 4320 conductivity meter at 298 K. The magnetic susceptibility measurements of the investigated complexes were evaluated at room temperature with a Gouy balance by making diamagnetic corrections using Pascal's constant.[1,2,6,7] The effective magnetic moments, μ_{eff}, per metal atom were calculated from the equation $\mu_{eff} = 2.83\sqrt{\chi'_M T}$, where χ'_M is the molar susceptibility. Infrared (IR) spectra of the ligand and its metal chelates were monitored using a Shimadzu model 8101 spectrometer in the region 400–4000 cm^{-1} using KBr discs with high resolution of 2 cm^{-1}. UV–visible spectra of the prepared ligand and its complexes were monitored using 10 mm matched quartz cells with a PG model T+80 spectrophotometer. Thermal analyses were recorded using a Shimadzu 60H for recording the thermodynamic curves (thermogravimetric analysis (TGA), differential thermogravimetry (DTG)) of the investigated solid compounds in nitrogen atmosphere (40 ml min^{-1}) at a heating rate of 10°C min^{-1} from ambient temperature to 750°C. The values of absorbance of the complexes of 4×10^{-5} mol dm^{-3} were measured at different pH values and were adjusted using a series of Britton universal buffer.[18] A HANNA211 pH meter was applied for pH measurements at 298 K.

Preparation of Schiff base ligand

The Schiff base ligand, namely *Z*-3-((2-((*E*)-(2-hydroxynaphthyl) methylene)amino)-5-nitrophenylimino)-1,3-dihydroindin-2-one (HL), was prepared as follows. 4-Nitro-*o*-phenylenediamine (5 mmol, 0.77 g) in 25 ml of ethanol was slowly added to ethanol solution (25 ml) containing isatin (5 mmol, 0.74 g) followed by slow addition of 2-hydroxy-1-naphthaldehyde (5 mmol, 0.86 g) dissolved in 25 ml of ethanol. A dark orange precipitate was obtained on refluxing the solution for 3 h.[19] The precipitate was filtered using suction and washed thoroughly with aqueous ethanol solution. The pure compound was dried in a desiccator over anhydrous calcium chloride. The structure of HL is shown in Scheme 1.

The physical and spectroscopic data for ligand HL are as follows. Dark orange; m.p. 228°C; yield 80%. ^{1}H NMR (400 MHz, DMSO-d_6, δ, ppm): 14.58 ppm (s, 1H, OH), 10.82 (s, 1H, CH N), 9.76 (s, 1H, H-C17), 8.94 (d, J = 8.5 Hz, 1H, H-C23), 8.64 (d, 1H, J = 9.1 Hz, H-C15), 8.19 (d, 1H, J = 9.1 Hz, H-C14), 8.14 (d, 1H, J = 8.0 Hz, H-C25), 8.05 (d, 1H, J = 8.5 Hz, H-C22,), 7.99 (d, 1H, J = 8.5 Hz, H-C28), 6.67 (dd, 1H, J = 8.0, 6.1 Hz, H-C26), 6.71 (dd, 1H, J = 8.5, 6.1 Hz, H-C27), 7.91 (d, 1H, J = 7.7 Hz, H-C6), 7.60 (dd, 1H, J = 7.7, 5.9 Hz, H-C7), 7.43 (dd, 1H, J = 8.5, 5.9 Hz, H-C8), 7.25 (s, 1H, NH), 7.23 (d, 1H, J = 8.5 Hz, H-C9). ^{13}C NMR (100 MHz, DMSO-d_6, δ, ppm) (Scheme 1): (C3) = 234.7, (C2) = 181.8, (C5) = 137.3, (C7) = 133.1, (C9) = 128.5, (C8) = 124.4, (C6) = 120.0, (C4) = 116.2, (C13) = 160.1, (C16) =149.8, (C12) = 148.2, (C15) = 121.6, (C14) = 124.1, (C17) = 121.4, (C19) = 168, (C21) = 163.7, (C24) = 160.1, (C23) = 133.3, (C29) = 133.1, (C25) = 128.5, (C27) = 127.9, (C28) = 113.8, (C26) = 113.9, (C22) = 111.4, (C20) = 110.5. Anal. Calcd for ($C_{25}H_{16}N_4O_4$) (%): C, 68.81; H, 3.67; N, 12.73. Found (%): C, 68.69; H, 3.55; N, 12.73. Selected IR data (KBr disc, cm^{-1}): 3437 (b), 3199 (m), 3021 (w), 3070 (w), 1740 (s), 1634 (vs), 1600 (s), 1212 (m).

Preparation of metal complexes

A solution of $Cu(CH_3COO)_2{\cdot}H_2O$ (1.00 g, 5 mmol, 30 ml of ethanol) or $Ni(NO_3)_2{\cdot}6H_2O$ (1.45 g, 5 mmol, 30 ml of ethanol) was added to a solution of HL (2.18 g, 5 mmol, 30 ml of ethanol). The resulting mixture was stirred and refluxed with stirring for 1 h. A dark brown precipitate in the case of copper and dark red precipitate in the case of nickel was formed, which was filtered off, washed with ethanol and dried *in vacuo* over anhydrous $CaCl_2$.

NiL. Dark red; m.p. > 300°C; yield 75%. Anal. Calcd for [Ni($C_{25}H_{17}N_5O_8$)]·½H_2O (%): C, 51.49; H, 2.92; N, 12.01. Found (%): C, 51.35; H, 2.77; N, 11.93. Molar conductance Λ_m (Ω^{-1} mol^{-1} cm^2) in DMF: 2.07. Selected IR data (KBr disc, cm^{-1}): 3468 (b), 3207 (m), 3056 (w), 3028 (w), 1699 (s), 1618 (vs), 1569 (s), 1167 (m), 668 (w), 575 (w).

CuL. Dark brown; m.p. > 300°C; yield 78%. Anal. Calcd for [Cu($C_{27}H_{20}N_4O_7$)]·H_2O (%): C, 54.59; H, 3.71; N, 9.43. Found (%): C, 51.48; H, 3.60; N, 9.31. Molar conductance Λ_m (Ω^{-1} mol^{-1} cm^2) in DMF: 4.46. Selected IR data (KBr disc, cm^{-1}): 3451 (b), 3199 (m), 3039 (w), 3050 (w), 1689 (s), 1600 (vs), 1570 (s), 1172 (m), 641(w), 581(w).

Magnetic moment measurements

Magnetic susceptibility measurements supply information to support the electronic structure of the investigated complexes.

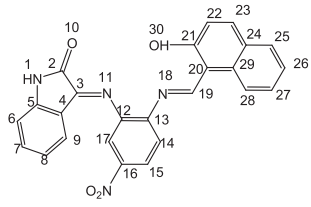

Scheme 1. Structural formula of the prepared Schiff base ligand HL.

Magnetic susceptibility was calculated according to the following relation:[1,2,7,20,21]

$$\mu_{\text{eff}} = 2.83\sqrt{\chi_{\text{M}}^{'}T} \quad (1)$$

$$\chi_{\text{M}}^{'} = \chi_{\text{M}} - (\text{diamag.corr.}) \quad (2)$$

where μ_{eff} is the magnetic moment (in Bohr magnetons), χ'_{M} the molar magnetic susceptibility, T the absolute temperature (K) and χ_{M} after correction.

Evaluation of stoichiometry of prepared complexes

The stoichiometry of the tested complexes was determined by applying the spectrophotometric molar ratio method[1,2,7,22] and continuous variation method,[5,6,24] as shown in Figs S4 and S5.

Evaluation of apparent formation constants of synthesized complexes

The apparent formation constants (K_{f}) of the synthesized complexes formed in solution were determined from spectrophotometric measurements using the continuous variation method,[2,5,20,25] according to the following relation:

$$K_{\text{f}} = \frac{A/A_{\text{m}}}{(1 - A/A_{\text{m}})^2 C} \quad (3)$$

where A is the arbitrarily chosen absorbance value on either side of the absorbance mountain col. (pass), C is the initial concentration of the metal and A_{m} is the absorbance at the maximum formation of the complex. The obtained K_{f} values (Table 1) indicate the stability of these complexes.

Kinetic studies of prepared complexes

Kinetic and thermodynamic studies of the thermal degradation process are a powerful tool for providing sufficient knowledge about Arrhenius parameters, i.e. frequency factor (A), entropy of activation (ΔS^*), enthalpy of activation (H^*) and free energy of activation (ΔG^*). From TGA/DTG curves, the Coats–Redfern method was employed to calculate the mentioned kinetic parameters:[6,7,26]

$$\log\left[\frac{\log(W_\infty/(W_\infty - W))}{T^2}\right] = \log\left[\frac{AR}{\varphi E^*}\left(1 - \frac{2RT}{E^*}\right)\right] - \frac{E^*}{2.303RT} \quad (4)$$

where W_∞ is the mass loss at the completion of the decomposition reaction, W is the mass loss up to temperature T, R is the universal gas constant and φ is the heating rate. Since $1 - 2RT/E^* \approx 1$, a plot of the left-hand side of equation (4) against $1/T$ would give a straight line. E^* was then calculated from the slope and the Arrhenius constant, A, was obtained from the intercept. The other kinetic parameters, S^*, H^* and G^*, were calculated using the following equations:

$$\Delta S^* = 2.303R \log\frac{Ah}{K_{\text{B}}T} \quad (5)$$

$$\Delta H^* = E^* - RT \quad (6)$$

$$\Delta G^* = H^* - T\Delta S^* \quad (7)$$

where K_{B} and h are Boltzmann's and Planck's constants, respectively.

Computational aspects

With the increasing development of computational chemistry, density functional theory (DFT) has been extensively utilized due to its accuracy and low computational cost to calculate a wide variety of molecular properties and it has provided authoritative results which are in accordance with experimental data. We attempted to reconnoitre the optimized geometrical parameters (bond lengths, bond angles and dihedral angles), net charges on active centres and energetics of the ground state for the unsymmetric tetradentate Schiff base ligand HL and its complexes with Ni(II) and Cu(II) metals. In all calculations, DFT was used at the B3LYP level,[27] 6-311G ++ (d, p)[28] as a basis set for the ligand and LANL2DZ[29] as a basis set for the complexes. All calculations were performed using the Gaussian 09 W program.[30]

Table 1. Electronic absorption spectral data, magnetic data, formation constant (K_{f}) and stability constant for the prepared Schiff base ligand and its complexes

Schiff base ligand/complex	λ_{max} (nm)	Assignment	μ_{eff} (BM)	Proposed geometry	K_{f}	Log K_{f}
HL	460	n → π*	—	—	—	—
	396	n → π*				
	314	π → π*				
	272	π → π*				
CuL	737 (b)[a]	d–d band	1.87	Octahedral	8.24×10^5	5.92
	512	d–d band				
	484	LMCT band				
	393	Intraligand band				
	325	π → π*				
NiL	741	d–d band	3.10	Octahedral	4.44×10^5	5.65
	550	d–d band				
	437	LMCT band				
	251	π → π*				

[a]b = broad

Biological activity

DNA studies

Electronic spectra

The interaction of the studied complexes with DNA was conducted in Tris–HCl buffer (50 mM, pH = 7.2) at room temperature to investigate the binding affinity between CT-DNA and the complexes. Before employing CT-DNA, it was purified by centrifugal dialysis. CT-DNA solution in the buffer solution at pH = 7.5 gives a ratio of UV absorbance >1.86 at 260 and 280 nm, indicating that the DNA was sufficiently free from protein contamination.[1,2,9,30,31] The concentration of CT-DNA per nucleotide was determined by observation the UV absorption at 260 nm using ε_{260} = 6600 mol^{-1} cm^2. The stock solution was stored at 4 °C and used within one day. Absorption titration was carried out by varying the concentration of CT-DNA (3–30 μM), while keeping the metal complex concentration (10^{-5} M) constant. The absorption of free CT-DNA was eliminated by adding equimolar CT-DNA to pure buffer solution in the reference compartment and the resulting spectra were believed to result from the metal complexes and the DNA–metal complex aggregates. The titration processes were repeated until there was no change in the spectra, indicating binding saturation had been achieved. The absorption data were estimated for an evaluation of the intrinsic binding constant (K_b) of the complexes with CT-DNA.[32]

Viscosity measurements

Viscosity experiments were accomplished using an Ostwald microviscometer and a water bath maintained at constant temperature (25 ± 1°C). The DNA concentration was kept constant in all samples, but the complex concentration was increased each time (10–250 μM). Mixing of the solution was achieved by bubbling nitrogen gas through viscometer. The mixture was left for 10 min at 37°C after addition of each aliquot of complex. The flow time was repeatedly measured with an accuracy of ±0.2 s with a digital stopwatch. Data are presented as $(\eta/\eta^0)^{1/3}$ versus the ratio [complex]/[DNA] = R, where η and η^0 are the specific viscosities of DNA in the presence and absence of complex, respectively. The values of η and η^0 were calculated using the following equation: $\eta = (t - t_o)/t_o$, where t_o is the observed flow time of DNA-containing solution and t is the flow time of buffer alone.[1,5–7,33,34] Relative viscosities of DNA were calculated from the ratio (η/η^0).

Agarose gel electrophoresis of DNA interaction with investigated complexes

Agarose was purchased from Fischer-Biotech (GC Health care). CT-DNA and Ready-load 100 bp DNA ladder were used as the native-size DNA and were purchased from Bio Labs. The samples were subjected to electrophoresis on 1% agarose gel prepared in TBE buffer (45 mM Tris, 45 mM boric acid and 1 mM EDTA; pH = 7.3), with 20 μl of each of the incubated complexes and 20 μl of DNA. The mixture was incubated at room temperature for 30 min at 37°C. After that, it was loaded on the gel with tracking dye (0.25% bromophenol blue). The electrophoresis was performed at constant voltage (100 V) for about 2 h (until the bromophenol blue had passed through 50% of the gel) in TBE buffer. At the end of electrophoresis, i.e. the end of DNA migration, the electric current was switched off. Then, the gel was stained by immersing it in water containing ethidium bromide (0.5 μg ml^{-1}) for 30–45 min at room temperature and later visualized under UV light using a transilluminator and photographed with a Panasonic DMC-LZ5 Lumix digital camera.[2,7,20,34]

Antimicrobial activity

The prepared Schiff base ligand and its complexes were screened for their bactericidal and fungicidal activities by agar and potato dextrose agar diffusion methods, respectively, against Staphylococcus aureus, Escherichia coli and *Pseudomonas aeruginosa* bacteria and *Aspergillus flavus*, Candida albicans and *Trichophyton rubrum* fungi. Each compound was dissolved at different concentrations of 10 and 25 mg ml^{-1} in DMSO solvent. The bacteria were sub-cultured in agar medium. Petri dishes were incubated for 24 h at 37°C. Standard antibacterial drug tetracycline was also tested under similar conditions for comparison. The fungi were sub-cultured in potato dextrose agar medium. Standard antifungal drug fluconazole was utilized for comparison. Petri dishes were incubated for 48–72 h at 35°C. The minimum inhibitory concentration for each tested substance was determined by microscopic observation of microbial growth. It corresponds to the well with the lowest concentration of the tested substance where microbial growth was clearly inhibited. The zones of inhibition based upon zone size around the wells were measured. The activities of the prepared complexes were determined by calculating the activity index (Table S5) according to the following relation:[1,2,20,35]

$$\text{Activity index } (A) = \frac{\text{Inhibition zone of complex (mm)}}{\text{Inhibition zone of standard drug (mm)}} \times 100 \quad (8)$$

Results and discussion

Characterization of Schiff base ligand

The tetradentate Schiff base ligand HL was prepared by the reaction of 4-nitro-*o*-phenylenediamine with isatin and 2-hydroxy-1-naphthaldehyde in ethanol. The structure of the ligand was confirmed using ^{1}H NMR, ^{13}C NMR, IR and UV–visible spectroscopies, elemental analysis and theoretical studies. The structure of the ligand is represented in Scheme 1. Unfortunately, single crystals of the studied ligand could not be obtained because of lack of solubility in most organic solvents.

^{1}H NMR and ^{13}C NMR spectra

The synthesized ligand was characterized from its ^{1}H NMR spectrum (400 MHz) in DMSO-d_6. The data are presented in the Experimental section and in Figs S1 and S2. All the spectra are in good agreement with the proposed structure of the ligand. The ^{1}H NMR spectrum of the synthesized Schiff base ligand shows distinguishing NMR signals. The spectrum of HL shows a singlet signal at 14.58 ppm for OH proton. The signal due to the azomethine proton (HC N) is found at 10.82 ppm. The ^{1}H NMR spectra of the complexes cannot be obtained due to interference of their paramagnetic properties.

Characterization of metal complexes

Elemental analyses and molar conductance measurements

Interaction of copper acetate and nickel nitrate with HL in ethanol gives dark brown and red powder complexes, respectively. The isolated solid complexes were characterized using elemental analyses,

IR and UV–visible spectroscopies, molar conductance, TGA and magnetic susceptibility. All complexes are stable in air at room temperature, non-hygroscopic, insoluble in water and soluble in polar coordinating solvents such as DMSO and DMF. The stoichiometries of the complexes derived from elemental analyses correspond to the general formula $[M(L)(X)(H_2O)]\cdot nH_2O$, where X = CH_3COO^- or NO_3^- and *n* = number of hydrated water molecules (Scheme 2). These proposals are also in accord with molar conductance, IR, TGA and UV–visible results.

Conductivity measurements have frequently been used in structure elucidation of metal chelates, i.e. the possible mode of bonding within the limit of their solubility; they also provide a method of testing the degree of ionization of complexes. The molar conductivities (Λ_m) of Cu(II) and Ni(II) complexes in DMF solution at 25 °C were measured. The low values of Λ_m reveal that the acetate and nitrate groups remain in the coordination sphere.[36]

IR spectroscopy

IR spectra of HL and its complexes were recorded in KBr pellets from 400 to 4000 cm^{-1}. These bands give fundamental information about the nature of the functional groups attached to the metal atoms.[37] The IR spectra of HL and its complexes are found to be quite complex as they in general exhibit a large number of bands of varying intensities. The spectrum of HL shows peaks of azomethine group CH N at 1634 and 1600 cm^{-1}, which are shifted to lower frequencies in the spectra of the complexes within the ranges 1600–1618 and 1569–1573 cm^{-1}. This result indicates that the nitrogen atom of the two CH N shares the coordination with metal ions.[1,2,7,20,26,37] The stretching vibration motion of indole (C O) in the free ligand is located at 1740 cm^{-1}, which is shifted to lower frequencies in the spectra of the complexes indicating the involvement of (C O) in the coordination.[31] The ligand shows a peak at 3199 cm^{-1} which is assigned to ν(NH) of amide group; upon complex formation this peak remains at the same frequency or slightly shifted from its position suggesting no participation of (NH) in bonding.[38] The appearance of a band at 3437 cm^{-1} in the IR spectrum of HL can be assigned to ν(OH). This band disappears in the spectra of the complexes but is replaced in the same place by other bands within 3451–3468 cm^{-1} assigned to the stretching motion of uncoordinated water molecules. The phenolic (C O) stretching vibration appears at 1212 cm^{-1} for the free ligand, shifted towards lower frequencies (1167–1172 cm^{-1}) for the complexes. This shift confirms the involvement of the oxygen atom of phenolic group in the chelation with C O M.[39] In the case of the metal complexes, there are number of medium to weak bands in the two ranges 641–668 and 475–581 cm^{-1} which are assigned to the ν(M O) and ν(M N) stretching frequencies, respectively. Two essentially strong to medium bands are seen at 1520 and 1341 cm^{-1} which can be assigned to ν_{asy}(COO) and ν_{sy}(COO) vibrations of carboxylate ion.[40] The difference between the asymmetric and symmetric stretching vibration motions $\Delta\nu$ (= ν_{asy}(COO) − ν_{sy}(COO)) is found to be 179 cm^{-1}, which matches with monodentate ligation.[41] The characteristic frequencies of the coordinating nitrate group in the nickel complex appear at 1423 cm^{-1} ($\nu(NO_2)_{asy}$), 1311 cm^{-1} ($\nu(NO_2)_{sy}$) and 1085 (ν(NO)). The difference between the two highest frequency bands ($\nu = \nu_{asy} - \nu_{sy}$) is 112 cm^{-1}, indicating that nitrate ion (NO_3) in the solid complex coordinates to Ni(II) ion in a unidentate manner.[42] These complexes also show weak bands at 820–890 cm^{-1} due to the presence of rocking mode of coordinated water molecules.[43] The presence of coordinated water is also established and supported from the TGA results for these complexes.

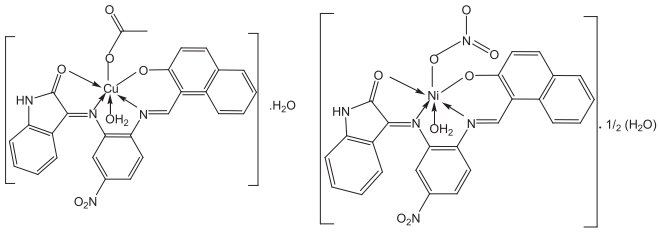

Scheme 2. Suggested structures of CuL and NiL.

Electronic spectra and magnetic properties of metal complexes

The UV–visible spectra of HL and its metal complexes were recorded in DMF solution at 298 K. Relevant electronic spectral data are presented in Table 1 and Fig S3. The UV–visible spectrum of HL shows three bands at 314, 396 and 460 nm. The first band at 314 nm is assigned to $\pi \rightarrow \pi^*$ transitions which are due to transitions from the benzene ring. The second band observed at 396 nm is most probably due to $n \rightarrow \pi^*$ transition for the electrons localized on the (C N) chromophore.[44] The third band observed at 460 nm is assigned to $n \rightarrow \pi^*$ transition originating from donating groups of the Schiff base ligand.[45] On complexation this band disappears, suggesting the coordination of azomethine nitrogen to the metal ion, as the formation of the metal–nitrogen bond stabilizes the electron pair on the nitrogen atom.[46]

Thus, addition of metal ion to ligand solution causes characteristic changes in the visible absorption spectrum of the ligand, suggesting an immediate complex formation in solution.[47] The designed complexes display a characteristic band centred at λ_{max} = 251–393 nm, due to an intramolecular charge transfer transition taking place in the complexed ligand. Moreover, there is a band appearing in the region 437–484 nm, which can be attributed to charge transfer from ligand to metal. Furthermore, the $d \rightarrow d$ transition band is observed from 515 to 741 nm. This band can be mainly attributed to transitions in an octahedral structure of the prepared complexes. The Cu(II) complex shows bands at 737 and 515 nm, which can be attributed to a $^2E_g \rightarrow {}^2T_g$ transition characteristic of tetragonally distorted octahedral geometry.[48] The Ni(II) complex exhibits two bands at 741 and 550 nm, attributed to $^3A_2g \rightarrow {}^3T_2g(F)$ and $^3A_2g \rightarrow {}^3T_2g(F)$ transition geometry around the Ni(II) ion.[49]

Magnetic measurements were recorded at room temperature. The effective magnetic moment (μ_{eff}) values of the complexes are given in Table 1. The μ_{eff} value at room temperature of the Ni(II) complex is 3.10 BM, which is in the normal range observed for octahedral Ni(II) complexes. This indicates that the Ni(II) complex is probably octahedral.[49] On the other hand, the μ_{eff} value (1.87 BM) for the Cu(II) complex falls within the range normally observed for tetragonally distorted octahedral Cu(II) complexes.[50]

Evaluation of stoichiometry of prepared Schiff base ligand complexes

The stoichiometry of the tested complexes was determined by applying the spectrophotometric continuous variation[2,20] and molar ratio methods.[5,6,20,23] The curves of continuous variation method display maximum absorption at mole fraction X_{ligand} = 0.56 for Ni (II) and Cu(II) complexes, which indicates the formation of 1:1 metal ion to ligand complexes as presented in Scheme 2. The maximum change will occur when the mole ratio of the reactants is close to the optimum ratio which is the stoichiometric ratio in the chemical

equation. Moreover, the data resulting from applying the molar ratio method support the same metal ion to ligand ratio of the prepared complexes (Figs S4 and S5).

Evaluation of apparent formation constants of synthesized complexes

The obtained apparent formation constants indicate the high stability of the prepared complexes. The values of K_f for the prepared complexes decrease according to the following sequence: CuL > NiL. Moreover, the values of log K_f (stability constant) of the investigated complexes are presented in Table 1.

Stability range of investigated complexes

The stability range of the studied complexes was found to be in the pH range of 4–10 for CuL and 4–11 for NiL according to the obtained pH–absorbance curves (Fig. S6). This means that M(II) ion greatly stabilizes the Schiff base in this range. Accordingly, these ligands can be used as masking reagents of M(II) ions in that range of pH.

Thermal analysis and kinetic and thermodynamic parameters of complexes

The thermal decomposition data for the two complexes are summarized in Table 2. The results show good agreement with the formulas suggested from the analytical data. TGA of Cu(II) and Ni(II) complexes exhibits a weight loss at 110 and 125°C, respectively, indicating the elimination of lattice water molecules from the complexes. Whereas the coordinated water molecules are removed at 215 and 220°C.[51] Then, the ligand decomposes gradually to the corresponding metallic residue at higher temperature. These results are consistent with the composition of the two complexes.

In continuation of the thermal investigation, the thermo-kinetic parameters of the decomposition steps for the metal complexes are listed in Table 2. From the obtained data, the following remarks can be made:

i. The S^* values for the complexes are found to be negative. This indicates that the activated complex is more ordered than the reactants and/or the reactions are slow.[52]
ii. The negative values of H^* mean that the decomposition processes are exothermic.
iii. The positive values of G^* for the investigated complexes reveal increases significant for the subsequently decomposition stages due to the increasing values of TS^* from one step to another which override the values of H^*. This increase reflects that the rate of removal of the subsequent ligand will be lower than that of the preceding ligand.[53]

Theoretical calculations

From the elemental analysis and spectroscopic data, Cu(II) and Ni(II) metals were expected to be coordinated to the ligand through a nitrogen atom (N1) and an oxygen atom (O9) forming a six-member ring, through a nitrogen atom (N1) and a nitrogen atom (N10) forming a five-member ring and through a nitrogen atom (N10) and an oxygen atom (O13) forming a five-member ring (Fig. 1).

Geometric parameters of ligand

The optimized structure of the ligand (anion), numbering system and vector of the dipole moment are depicted in Fig. 1(a). The energy of the highest occupied molecular orbital E_{HOMO}, energy of the lowest unoccupied molecular orbital E_{LUMO}, energy gap E_g and the dipole moment computed by B3LYP/6-311G++(d, p) for the neutral ligand and its anion are presented in Table S1. In addition, the computed geometric parameters were compared with the corresponding values obtained from the experimental data. The optimized bond length (Table S3) of C C in phenyl rings of the ligand falls in the range 1.379–1.425 Å which is greater than the experimentally determined value of 1.339 Å; for the C O bond, the optimized length of 1.236 Å is slightly shorter than the experimental value of 1.243 Å; and the optimized C N bond length of the ring fall in the range 1.397–1.399 Å which is shorter than the experimental value of 1.344 Å.[54] The bond angles for DFT-B3LYP/6-311G++(d, p) reported are slightly better than those for the HF method compared to the experimental results. The computation underestimates the ∠NCC and ∠OCO angles. The ligand and its anion are non-planar with naphthyl and indolin-2-one moieties out of the molecular plane of the 5-nitrophenyl ring by 55°. The differences between calculated and measured values

Table 2. Thermal, kinetics and thermodynamic parameters for metal complexes

Compound	T (°C)[a]	Weight loss (%)[b]	Proposed segment	E^* (kJ mol^{-1})	A (× 10^4 s^{-1})	H^* (kJ mol^{-1})	S^* (kJ mol^{-1} K^{-1})	G^* (kJ mol^{-1})
CuL	35–110	3.05 (3.03)	H_2O	0.11	0.71	−1.06	−0.167	22.43
	110–215	3.06 (3.03)	H_2O			−1.36	−0.169	28.75
	215–367	9.96 (9.94)	CH_3COO			−2.22	−0.171	45.87
	367–513	28.50 (28.47)	$C_{11}H_7NO$			−3.33	−0.173	68.71
	459–749	44.90 (44.82)	$C_8H_5N_2O + C_6H_3NO_2$			−3.78	−0.174	78.14
Final residue (%)[c]	>749	10.53 (10.71)	Cu					
NiL	39–125	1.60 (1.54)	$0.5H_2O$	0.11	1.93	−1.63	−0.159	31.96
	125–222	3.20 (3.09)	H_2O			−1.61	−0.161	38.19
	222–395	10.82 (10.64)	NO_3			−1.64	−0.164	55.60
	395–478	24.94 (24.88)	$C_8H_5N_2O$			−1.65	−0.165	61.77
	478–566	29.11 (29.00)	$C_{11}H_7NO$			−1.66	−0.166	72.69
	566–749	20.05 (20.77)	$C_6H_3NO_2$			−1.69	−0.169	102.97
Final residue (%)[c]	>749	10.28 (10.08)	Ni					

[a]Temperature range of decomposition pathways
[b]Weight loss found (calculated)
[c]Residue found (calculated)

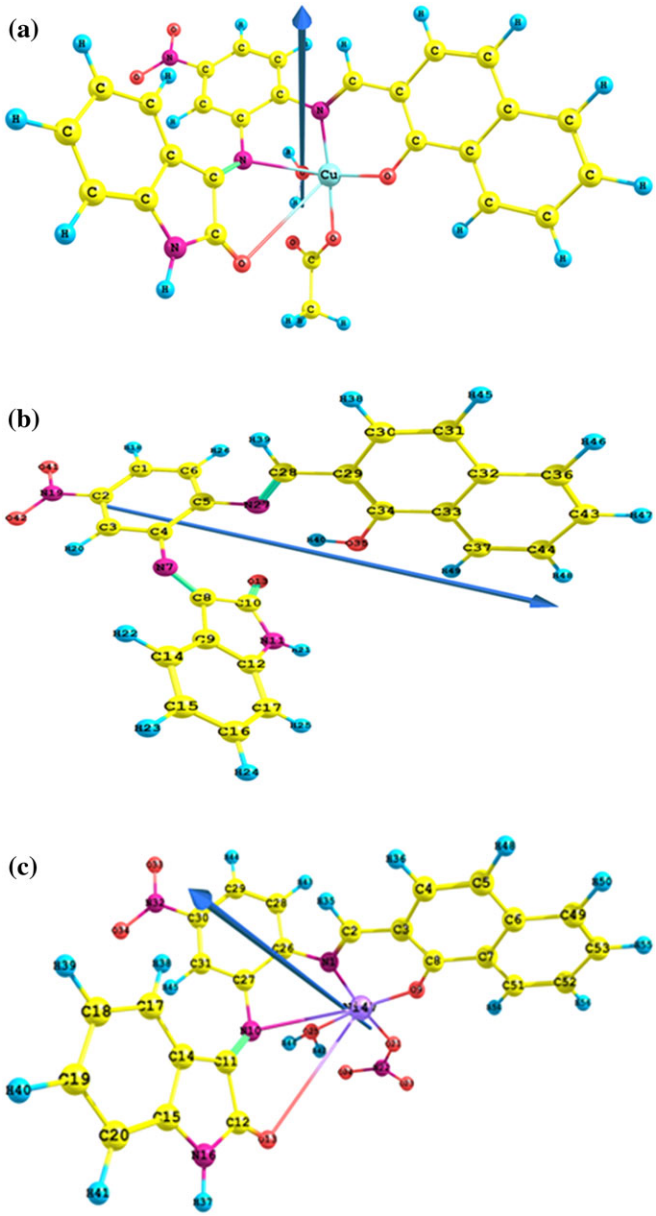

Figure 1. Optimized geometry, numbering system and vector of the dipole moment of compounds using B3LYP/6-31G++(d, p): (a) Schiff base ligand anion; (b) NiL complex; (c) CuL complex.

can be explained by the fact that the calculations assume an isolated molecule where the intermolecular columbic interactions with neighbouring molecules are absent, where the experimental results correspond to interacting molecules in the crystal lattice for a similar compound. The ligand in its anion form is considered as the most electron-donating as indicated from computed E_{HOMO} (Table S1). The computed energy gap E_g, which measures the reactivity, shows that free ligand in its anion form is the most reactive ligand (smallest value). The computed dipole moment shows that the anion form of the ligand is less polar than the neutral form by 1.33 D (Table S1). From the computed net charge on active centres of the ligand, free ligand in its anion form, it is found that the most negative centres are N27, O35, N7 and O13 which are the centres chelated with the metal to form the complex.

Geometric parameters of complexes

Tables S1–S3 and Figs 1(b) and (c) present the optimized geometry, numbering system, vector of the dipole moment, energetics, dipole moment, energy gap, net charges on active centres, bond lengths, bond angles and dihedral angles of all metal complexes studied in this work. The electronic configuration for Ni(II) is $3d^8$ and for Cu(II) is $3d^9$. In all complexes, the metal ion coordinates with N1 and O9 to form a six-member ring and with N10 and O13 to form a five-member ring. Therefore, distortion from regular octahedral geometry is expected for all the studied complexes.

The geometric changes that are observed in the ligand moiety itself are interesting. Thus, most bonds show elongation upon complexation with the metal ion. The length of the coordinate covalent bonds between metal and ligand site, i.e. M N and M O, are too long compared to the typical M X bond lengths which have the values Cu O 1.62 Å, Cu N 1.66 Å and Ni N 1.44 Å.[54] The too long M O and M N bonds in the complexes mean that the ionic character of these bonds is small. Also, the charge on the metal ion in the complex is much less than 2 in Ni(II) and Cu(II); hence, the comparison between the calculated (B3LYP/6-31G++(d, p) and the typical M (II) N and M(II) O is not very precise.

The calculated values of bond angles (between metal ion and binding sites) (Table S3) O9MN1, N1MO25, O25MN10, N10MO13 and O13MO21 vary between 85° and 132° which compare nicely with the experimental data as obtained from X-ray analysis for O_h Cu complexes,[54] which indicate a distorted octahedral geometry. The values of the dihedral angles around metal ion, i.e. MN2C28C30, MO14C13N17, MO23N24O25 and MO10C9C4 (Table S3), are far from 0° or 180° which indicate that the metal ion is not in the same plane as the donating sites. All the studied complexes are polar, as is evident from the magnitudes of their dipole moment (Table S1). As the energy gap of the studied complexes decreases, the reactivity of the complexes increases. The reactivity of the Cu(II) complex is greater than that of the Ni(II) complex.

Charge distribution analysis

In the NiL and CuL complexes, Ni and Cu metal ions end up with net charges of 0.5562 and 0.6772 indicating that the two metal ions receive 1.4438 e and 1.3228 e from the surrounding ligand, respectively. This donation takes place mainly through the σ-orbital. The amount of electronic charge received by each metal ion in the studied complexes is presented in Table S2. The relative charges accumulated on each metal ion in the complexes are expected in terms of the size and electronegativity of the metal ion. There is no electron back-donation from the metal ion to the donating sites (O9, O13, N1 and N10) as indicated from the net charge on the donating sites before and after complexation (Table S2).

Biological evaluation of synthesized complexes

DNA binding studies

Electronic spectral studies

The interactions of metal complex with DNA have been a topic of interest for the development of effective chemotherapeutic agents. Transition metal centres are particularly attractive moieties for such research since they exhibit well-defined coordination geometries and also often have distinctive electrochemical or photophysical

properties, thus enhancing the functionality of the binding agent. Currently, the spectrophotometric method for DNA interaction appears to be the most commonly used for determination of DNA-binding constants of metal complexes.

Transition metal complexes can bind to DNA via covalent (replacement of a labile ligand of the complex by a nitrogen base of DNA, e.g. guanine N7) and/or non-covalent (intercalation, electrostatic or groove binding) interactions.[55] The binding of an intercalative complex molecule to DNA has been well elucidated by notable intensity decrease (hypochromism) and shift of the electronic spectral bands because of strong stacking interaction between the aromatic chromophore of the ligand and DNA base pairs. The degree of hypochromism and the amount of the shift depend on the strength of the intercalative interaction.[56] On the other hand, metal complexes which do not intercalate or interact electrostatically with DNA may exhibit hyperchromism.[57] Fixed amounts (10^{-5} M) of metal complexes were titrated with increasing amounts of CT-DNA in the range from 3 to 30 μM. The electronic spectra of the Cu(II) complex in the absence and presence of CT-DNA are shown in Fig. 2(a). The sharp bands at about 246 nm are assigned to intraligand π–π* transitions and the lowest energy bands at about 403 nm are attributed to the metal-to-ligand charge transfer transitions. The absorption spectra show clearly that the addition of DNA to the Cu(II) complex yields a significant hypochromism and a slight blue shift at the ligand-to-metal charge transfer (LMCT) band. Distinctly, these spectral characteristics suggest that all compounds have some interaction with DNA. These spectral characteristics indicate that the complex interacts with DNA most likely through a mode that involves electrostatic or hydrophobic interaction. As stated before, CuL complexes have a replaceable acetate ligand in solution, which may be replaced with H_2O molecules in solution.[58] So the complex contains a positive charge on the copper atom in the middle. Due to the removal of acetate ligand from the complex in solution, the CuL complex will have a flat part in the middle (tetradentate square planar). Therefore, possible interaction of the Cu(II) complex with DNA could be as follows (Scheme 3):

- First, interaction of Cu(II) complex with base backbone of DNA or even coordination of Cu^{2+} with base pairs of DNA.
- Second, insertion of the flat part of the complex between the base pairs and consequently coordination of Cu^{2+} with base pairs of DNA.

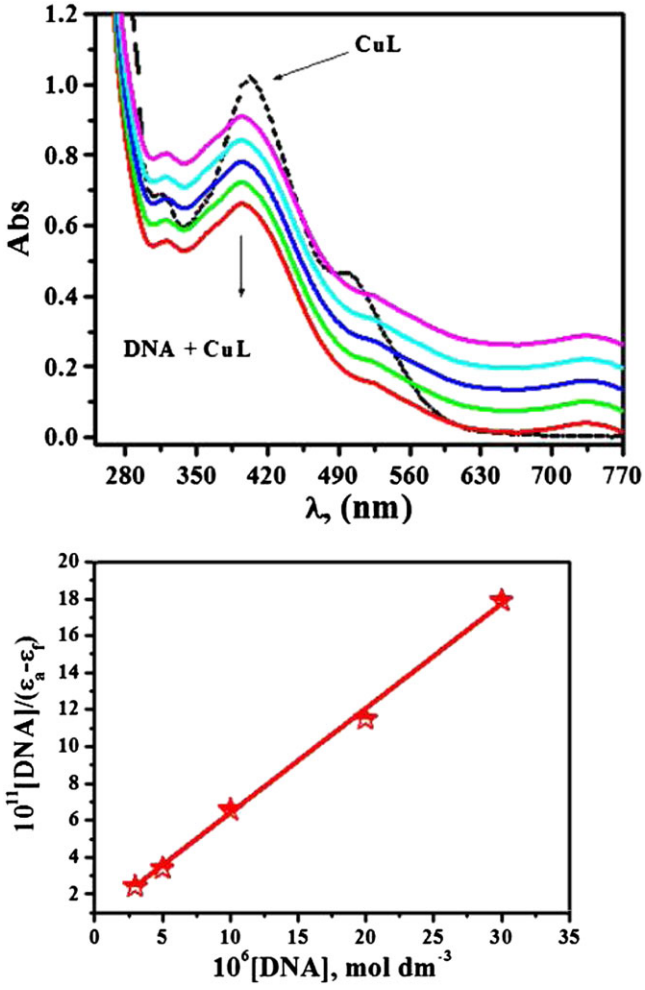

Figure 2. (a) Spectrophotometric titration of CuL complex (10^{-5} M) in 0.01 M Tris buffer (pH = 7.4, 25 °C) with CT-DNA from 3 to 30 μM. The arrow indicates increasing amount of DNA. (b) Plot of [CT-DNA]/($\varepsilon_a - \varepsilon_f$) versus [CT-DNA] for the titration of CT-DNA with CuL complex.

In order to quantitatively compare the binding affinity of the compounds with CT-DNA, the intrinsic binding constants (K_b) of the compounds were determined by monitoring the changes occurring in absorption at the LMCT band of the Cu(II) complex with increasing concentration of CT-DNA using the following functional equation:[1,2,7,20]

$$\frac{[DNA]}{\varepsilon_a - \varepsilon_f} = \frac{[DNA]}{\varepsilon_b - \varepsilon_f} + [K_b(\varepsilon_b - \varepsilon_f)]^{-1} \quad (9)$$

where [DNA] is the concentration of DNA in M^{-1} (nucleotide), ε_a is the molar absorption coefficient of the compound at a given DNA concentration, ε_f is the molar absorption coefficient of the compound in free solution, ε_b is the molar absorption coefficient of the compound when fully bound to DNA and K_b is the equilibrium binding constant in M^{-1}. In a plot of [DNA]/($\varepsilon_a - \varepsilon_f$) versus [DNA] (Fig. 2(b)), K_b is given by the ratio of the slope to the intercept. The K_b values of Ni(II) and Cu(II) complexes are determined to be 1.06×10^6 and 2.15×10^6 M^{-1}, respectively. However, the determined K_b values are higher than those observed for typical classical intercalators (ethidium bromide: $K_b = 1.4 \times 10^6$ M^{-1} in 25 mM Tris–HCl/40 mM NaCl buffer, pH = 7.2).[59] Hence, it is obvious that the present metal complexes are involved in strong intercalative interactions.

Viscosity studies

Although spectral techniques are necessary, they are not sufficient to support a binding mode. In the absence of crystallographic structural data, hydrodynamic measurements are considered as least obscure and the most critical test for determining the binding mode of DNA with small molecules.[60] Viscosity measurements are sensitive to changes in the DNA molecule. The sensitivity of this method largely relies on the changes in the DNA length that occur as result of its different binding modes with guest molecules. In classical intercalations, the DNA helix lengthens as base pairs are disconnected to accommodate the bound guest leading to increasing DNA viscosity,[1,2,61] whereas in groove binding or electrostatic mode, the length of the helix is unchanged resulting in no apparent alteration in DNA viscosity. In contrast, compounds that bind

Applied Organometallic Chemistry

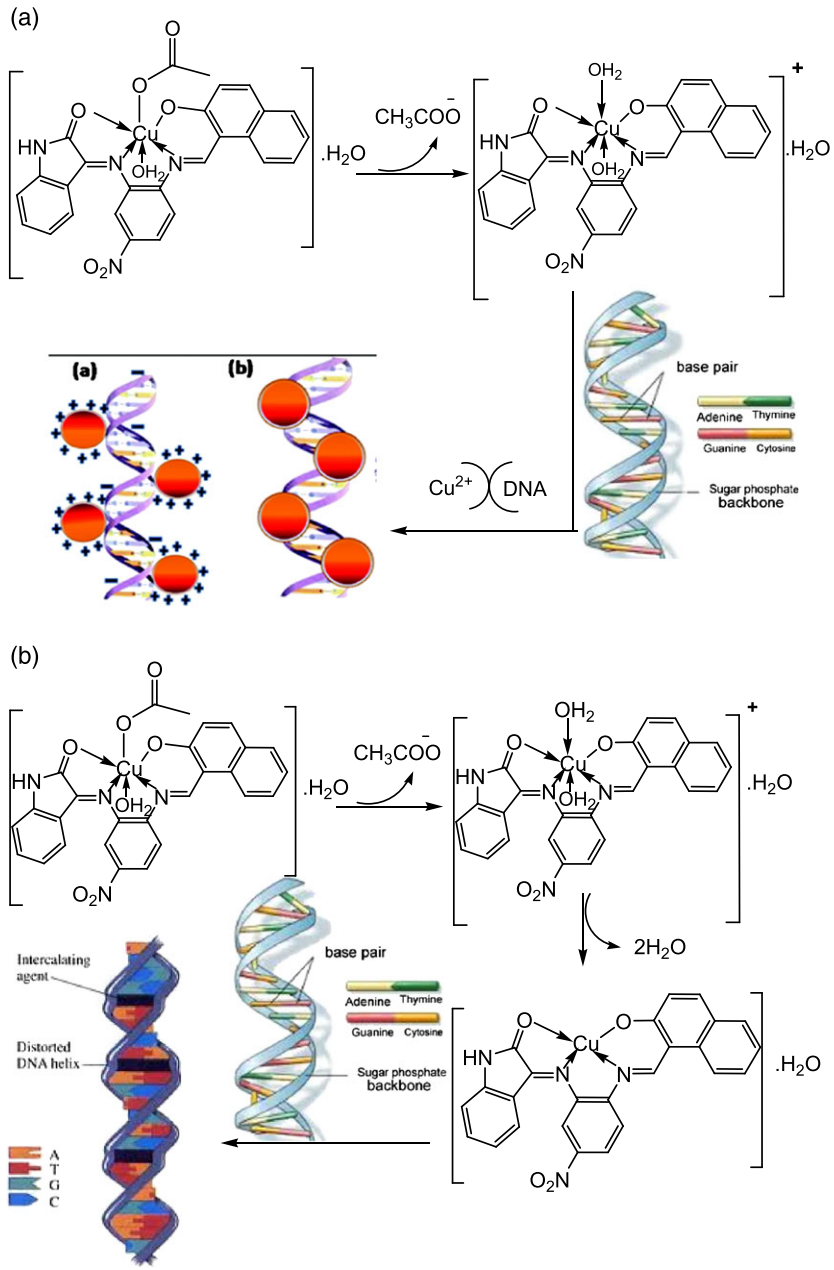

Scheme 3. Suggested mechanism for interaction of CuL with DNA (a) via electrostatic binding and (b) via intercalation binding.

exclusively in the DNA groove by partial and/or non-classical intercalation under the same conditions, typically give rise less pronounced or no change in the DNA solution viscosity.[62] A classical intercalation mode causes a significant increase in viscosity of DNA due to an increase in separation of base pairs at intercalation sites and hence an increase in overall DNA length. In order to further clarify the nature of the interaction between the complexes and DNA, viscosity measurements were carried out and are shown in Fig. 3. Plots of relative viscosity $(\eta/\eta_0)^{1/3}$ versus [complex]/[DNA] ratio (0–0.6) illustrate a significant increase in the relative viscosity of DNA on increasing concentration of complex, which is similar to that for intercalator ethidium bromide.[20,26] This may be explained by the insertion of the complexes between base pairs at intercalation sites and thus an increase in overall DNA length. On the basis of viscosity results, the compounds bind with DNA through intercalation mode. The increased degree of viscosity which may depend on affinity to DNA follows the order CuL > NiL. Thus, the viscosity measurements are consistent with the results of electronic spectra.

Gel electrophoresis

Gel electrophoresis is a widely used technique for studying the binding of compounds with nucleic acids: in this method separation of molecules will be on the basis of their relative rate of movement through a gel under the influence of an electric field. DNA is negatively charged and when it is placed in an electric field, it migrates towards the anode; the extent of migration of DNA is

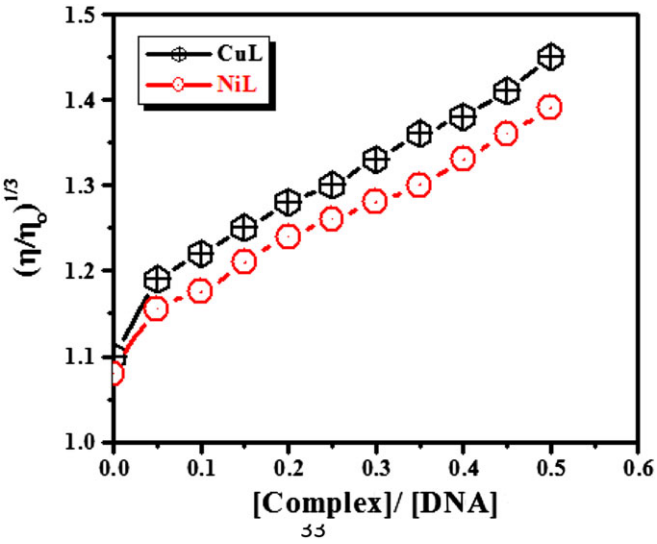

Figure 3. Effect of increasing amount of synthesized complexes on relative viscosities of DNA at [DNA] = 0.5 mM at 298 K.

determined by the strength of the electric field, buffer, density of agarose gel and size of DNA. Generally it is seen that mobility of DNA is inversely proportional to its size. Photographs of the gel show bands with different band widths and brightnesses compared to the control. The interaction of the prepared complexes with DNA was studied by agarose gel electrophoresis and the results are represented in Fig. 4 (lanes 2 and 3 are CT-DNA + metal complex; while lanes 1 and 4 are CT-DNA and blank). The diversity in DNA-cleavage efficiency of the investigated complexes is attributed to their difference in binding ability to DNA.[20,63] The intensity of lanes is decreased in the sequence CuL > NiL and these results are in a good agreement with values of binding constant of the tested complexes with CT-DNA (Table 3).

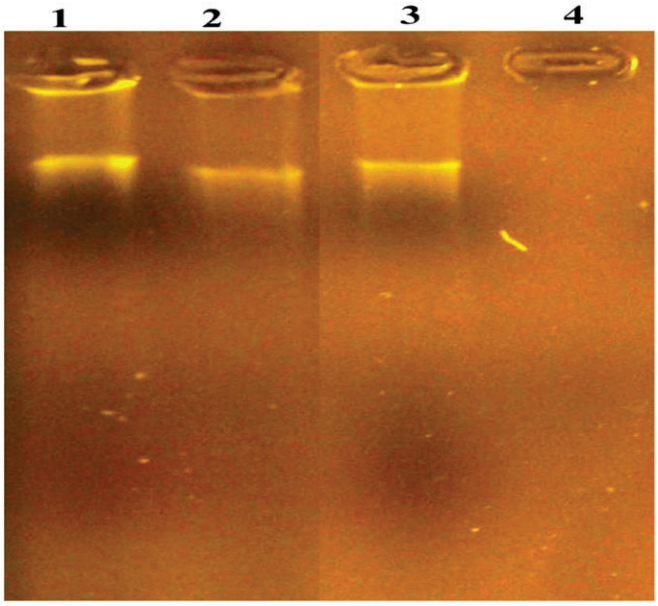

Figure 4. Gel electrophoresis pattern showing the interaction of the investigated complexes with DNA. Lane 1: CT-DNA; lane 2: CT- DNA + CuL; lane 3: CT-DNA + NiL; lane 4: blank.

Table 3. Spectral parameters for DNA interaction with the prepared complexes

Complex	λ_{max} (free) (nm)	λ_{max} (bound) (nm)	n	K_b ($\times 10^6$ M^{-1})	Type of chromism	Chromism (%)[a]	G^* (kJ mol^{-1})
NiL	245	243	2	1.00	hypo	32.80	−33.51
	465	439	26		hypo	60.75	−36.81
CuL	246	243	1	2.15	hypo	11.15	−33.51
	403	401	2		hypo		−36.12
						36.26	

[a]Chromism (%) = $(A_{free} - A_{bound})/A_{free}$

Antimicrobial activity

The free ligand and metal complexes were tested against bacterial and fungal species by measuring the size of the bacteriostatic diameter. The results are presented in Table S4, and it is evident that the tested compounds show marked bactericidal and fungicidal activities against various types of bacteria (S. aureus, E. coli and P. aeruginosa) and fungi (A. flavus, C. albicans and T. rubrum).

Antibacterial activity

The evolution of new bacterial strains resistant to current antibiotics has become critical problem in public health. Therefore, there is a strong stimulus to develop new bactericides. So, nowadays pharmaceutical industries are seeking for alternative compounds which behave as drugs. Currently much attention has been focused on the synthesis of new metal complexes and estimating their antibacterial activity. In the present work, we explored the activity of the Schiff base ligand and its metal(II) complexes against three different human pathogens. The diameter of the zone of inhibition (mm) was used to contrast the antimicrobial activity of the complexes with that of a commercial drug (tetracycline). The results show that complexes exhibit varying degrees of inhibitory effects on the growth of bacterial strains, which may be due to the effect of the metal ion on cell metabolism. Even though DMSO is an antimicrobial solvent, here we performed our antibacterial tests by employing DMSO as a negative control. Further, control experiments using DMSO alone do not show any antibacterial effect. Hence, it is noticed that the complexes are more potent bactericides than the free Schiff base. This higher antimicrobial activity of the metal complexes compared to the Schiff base may be due to the alteration in structure due to coordination and chelating tends to make metal complexes act as more powerful and potent bacteriostatic agents, thus blocking the growth of the microorganisms.[6,20,27,63] Moreover, coordination reduces the polarity of the metal ion mainly because of the partial sharing of its positive charge with the donor groups within the chelate ring system created during the coordination.[64] This process, in turn, increases the lipophilic nature of the central metal atom, which supports its permeation more efficiently through the lipid layer of microorganisms, thus destroying them more aggressively. The results (Table S4; Fig. 5) show that the Cu(II) complex has higher antibacterial activity than the Ni(II) complex. The diversity in the activity of the complexes against different microorganisms depends either on the impermeability of the cells of the microbes or differences in ribosomes in microbial cells.

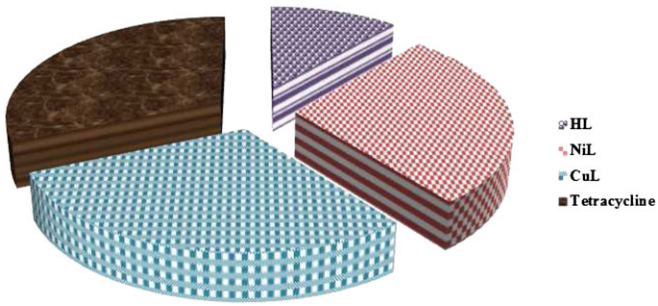

Figure 5. Antibacterial data of Schiff base ligand and its complexes against Staphylococcus aureus at 25 mg ml^{-1}.

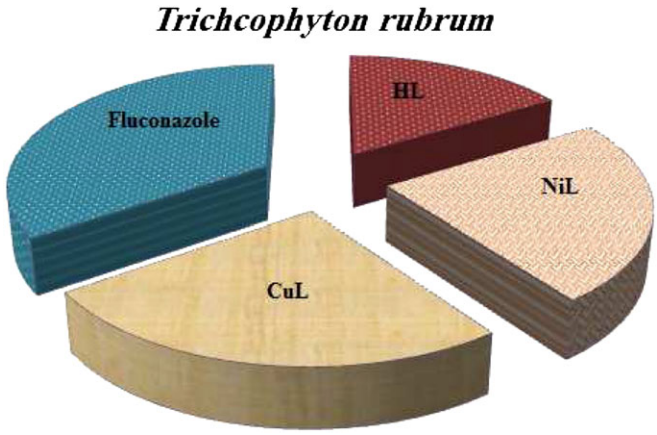

Figure 6. Antifungal data of Schiff base ligand and its complexes against *Trichophyton rubrum* at 25 mg ml^{-1}.

Antifungal activity

To provide a medicinal scope in the field of bioinorganic chemistry, the synthesized metal complexes were evaluated for their antifungal actions. The compounds were screened *in vitro* in order to find antifungal activity against A. flavus, C. albicans and T. rubrum species. The results of the antifungal studies are presented in Table S4 and Fig. 6 which reveal that the metal complexes are more toxic than the free ligand against the same organisms. Moreover, CuL has higher antifungal activity than NiL. From the results, it is observed that the fungal activity depends upon the nature of the metal ion. According to a literature survey concerning the antimicrobial activity of Schiff base complexes, we found that the studied complexes are more reactive.[1,2,27,65]

Conclusions

A new chelating agent and its complexes with Ni(II) and Cu(II) ions have been prepared and characterized. Analytical and spectral data revealed that the ligand was coordinated to the central metal ions by its two imine nitrogen atoms, phenolic oxygen atom and carbonyl group with 1:1:1 stoichiometry. Spectral characterization of the novel complexes showed that Cu(II) and Ni(II) ions with HL ligand form octahedral complexes where the ligand acts as a tetradentate one. Geometry optimization and conformational analysis have been performed and the model agreement with spectral data allow for suggesting the exact structure of the complexes. The stability of the complexes was discussed and kinetic parameters (E^*, A, ΔH^*, ΔS^* and ΔG^*) of all thermal decomposition stages have been estimated using the Coats–Redfern method. The synthesized complexes interact with DNA via intercalation mode and exhibited higher binding constant than a classical intercalator. The antimicrobial screening assay of the compounds revealed variable activities towards the studied bacterial and fungal organisms.

References

[1] L. H. Abdel-Rahman, R. M. El-Khatib, L. A. E. Nassr, A. M. Abu-Dief, F. E. Lashin, *Spectrochim. Acta A* **2013**, *111*, 266.
[2] L. H. Abdel-Rahman, R. M. El-Khatib, L. A. E. Nassr, A. M. Abu-Dief, A. A. Seleem, *Spectrochim. Acta A* **2014**, *117*, 366.
[3] J. P. Costes, S. Shova, W. Wernsdorfer, *J. Chem. Soc. Dalton Trans.* **2008**, 1843.
[4] X. G. Ran, L. Y. Wang, Y. C. Lin, J. Hao, D. R. Cao, *Appl. Organometal. Chem.* **2010**, *24*, 741.
[5] L. H. Abdel-Rahman, R. M. El-Khatib, L. A. E. Nassr, A. M. Abu-Dief, *J. Mol. Struct.* **2013**, *1040*, 9.
[6] L. H. Abdel Rahman, A. M. Abu-Dief, N. A. Hashem, A. A. Seleem, *Int. J. Nanomater. Chem.* **2015**, *1*, 79.
[7] L. H. Abdel-Rahman, A. M. Abu-Dief, S. K. Hamdan, A. A. Seleem, *Int. J. Nanomater. Chem.* **2015**, *1*, 65.
[8] A. Chakraborty, P. Kumar, K. Ghosh, P. Roy, *Eur. J. Pharmacol.* **2010**, *647*, 1.
[9] J. Gradinaru, A. Forni, V. Druta, F. Tessore, S. Zecchin, S. Quici, N. Garbalau, *Inorg. Chem.* **2007**, *46*, 884.
[10] B. J. Coe, N. R. M. Curati, *Inorg. Chem.* **2004**, *25*, 147.
[11] R. Atkins, G. Brewer, E. Kokot, G. M. Mockler, E. Sinn, *Inorg. Chem.* **1985**, *24*, 127.
[12] E. Kwiatkowski, M. Kwiatkowski, *J. Chem. Soc. Dalton Trans.* **1985**, 803.
[13] S. Saha, R. K. Kottalanka, P. Bhowmik, S. Jana, K. Harms, T. K. Panda, S. Chattopadhyay, H. P. Nayek, *J. Mol. Struct.* **2014**, *1061*, 26.
[14] J. R. Thakkar, N. V. Thakkar, *Synth. React. Inorg. Met. Org. Chem.* **2000**, *30*, 1871.
[15] N. R. Penthala, T. R. Yerramreddy, N. R. Madadi, P. A. Crooks, *Bioorg. Med. Chem. Lett.* **2010**, *20*, 4468.
[16] S. N. Pandeya, S. Smitha, M. Jyoti, S. K. Sridhar, *Acta Pharma.* **2008**, *66*, 43.
[17] Z. H. Chohan, H. Pervez, A. Rauf, *J. Enz. Inhib. Med. Chem.* **2004**, *19*, 417.
[18] H. T. S. Britton, *Hydrogen Ions*, 4th ed, Chapman and Hall, London, **1952**.
[19] V. P. Singh, S. Singh, D. P. Singh, *J. Enz. Inhib. Med. Chem.* **2012**, *27*, 319.
[20] A. M. Abu-Dief, L. A. E. Nassr, *J. Iran. Chem. Soc.* **2015**, *12*, 943.
[21] A. S. El-Tabl, F. A. El-Saied, A. N. Al-Hakimi, *J. Coord. Chem.* **2008**, *61*, 2380.
[22] P. K. Sharma, S. N. Dubey, *Ind. J. Chem.* **1994**, *33A*, 1113.
[23] H. M. Abd El-Lateef, A. M. Abu-Dief, B. E. M. El-Gendy, *J. Electroanal. Chem.* **2015**, *758*, 135.
[24] L. H. Abdel-Rahman, A. M. Abu-Dief, R. M. El-Khatib, S. M. Abdel-Fatah, *J. Photochem. Photobiol. B, Biol.* **2016**, *162*, 298.
[25] L. H. Abdel-Rahman, R. M. El-Khatib, L. A. E. Nassr, A. M. Abu-Dief, *Int. J. Chem. Kin. A* **2014**, *46*, 543.
[26] a) A. W. Coats, I. P. Redfern, *Nature* **1964**, *20*, 68. b) L. H. Abdel-Rahman, A. M. Abu-Dief, E. F. Newair, S. K. Hamdan, *J. Photochem. Photobiol. B* **2016**, *160*, 18.
[27] A. D. Becke, *J. Chem. Phys.* **1993**, *98*, 5648.
[28] M. P. McGrath, C. Radom, *J. Chem. Phys.* **1991**, *94*, 511.
[29] P. J. Hay, W. R. Wadt, *J. Chem. Phys.* **1985**, *82*, 299.
[30] M. J. Frisch, G. W. Trucks, H. B. Schlegel, G. E. Scuseria, M. A. Robb, J. R. Cheeseman, G. Scalmani, V. Barone, B. Mennucci, G. A. Petersson, H. Nakatsuji, M. Caricato, X. Li, H. P. Hratchian, A. F. Izmaylov, J. Bloino, G. Zheng, J. L. Sonnenberg, M. Hada, M. Ehara, K. Toyota, R. Fukuda, J. Hasegawa, M. Ishida, T. Nakajima, Y. Honda, O. Kitao, H. Nakai, T. Vreven, J. A. Montgomery, Jr., J. E. Peralta, F. Ogliaro, M. Bearpark, J. J. Heyd, E. Brothers, K. N. Kudin, V. N. Staroverov, R. Kobayashi, J. Normand, K. Raghavachari, A. Rendell, J. C. Burant, S. S. Iyengar, J. Tomasi, M. Cossi, N. Rega, J. M. Millam, M. Klene, J. E. Knox, J. B. Cross, V. Bakken, C. Adamo, J. Jaramillo, R. Gomperts, R. E. Stratmann, O. Yazyev, A. J. Austin, R. Cammi, C. Pomelli, J. W. Ochterski, R. L. Martin, K. Morokuma, V. G. Zakrzewski, G. A. Voth, P. Salvador, J. J. Dannenberg, S. Dapprich, A. D. Daniels, Ö. Farkas, J. B. Foresman, J. V. Ortiz, J. Cioslowski, D. J. Fox, *Gaussian 09*, Gaussian Inc., Wallingford, CT, **2009**.

[31] L. P. Nitha, R. Aswathy, N. E. Mathews, B. S. Kumari, K. Mohanan, *Spectrochim. Acta A* **2014**, *118*, 154.
[32] C. N. Sudhamani, H. S. B. Naik, D. Girija, K. R. S. Gowda, M. Giridhar, T. Arvinda, *Spectrochim. Acta A* **2014**, *118*, 271.
[33] S. Satyanarayana, J. C. Dabroniak, J. B. Chaires, *Biochemistry* **1992**, *31*, 9319.
[34] M. Vujcic, S. Tufegdzic, Z. Vujcic, M. J. Gašic, D. Sladic, *J. Serb. Chem. Soc.* **2007**, *72*, 1265.
[35] S. Gopalakrishnan, R. Rajameena, E. Vadivel, *Int. J. Pharm. Sci. Drug Res.* **2012**, *4*, 31.
[36] W. L. Geary, *Coord. Chem. Rev.* **1971**, *7*, 81.
[37] S. Brooker, S. S. Iremonger, P. G. Plieger, *Polyhedron* **2003**, *22*, 665.
[38] K. Nakamoto, *Infrared and Raman Spectra of Inorganic and Coordination Compounds*, 4th ed, Wiley Interscience, New York, **1993**.
[39] S. Sarawat, G. S. Srivastava, R. C. Mehrotra, *J. Organomet. Chem.* **1977**, *129*, 155.
[40] K. Nakamoto, *Infrared Spectra of Inorganic and Coordination Compounds*, Wiley, New York, **1970**.
[41] A. Z. El-Sonbati, M. A. Diab, M. S. El-Shehawy, M. Moqbal, *Spectrochim. Acta A* **2010**, *75*, 394.
[42] K. Nakamoto, *Infrared and Raman Spectra of Inorganic and Coordination Compounds, Part B*, 5th ed, Wiley, New York, **1985**, p. 87.
[43] K. Nakamoto, *Infrared Spectra of Inorganic and Coordination Compounds*, 3rd ed, Wiley Interscience, New York, **1970** , pp., p. 159 .167, 214
[44] O. A. M. Ali, *Spectrochim. Acta A* **2014**, *132*, 52.
[45] O. A. M. Ali, S. M. El-Medani, M. R. Abu Serea, A. S. S. Sayed, *Spectrochim. Acta A* **2015**, *136*, 651.
[46] M. Asadi, Z. Asadi, N. Savaripoor, M. Dusek, V. Eigner, M. R. Shorkaei, M. Sedaghat, *Spectrochim. Acta A* **2015**, *136*, 625.
[47] A. D. Khalaji, S. M. Rad, G. Grivani, D. Das, *J. Therm. Anal. Calorim.* **2011**, *103*, 747.
[48] A. A. El-Asmy, T. Y. Al-Ansi, R. R. Amine, M. M. Mounir, *Polyhedron* **1990**, *9*, 2029.
[49] S. A. Patil, S. N. Unki, A. D. Kulkarni, V. H. Naik, P. S. Badami, *Spectrochim. Acta A* **2011**, *79*, 1128.
[50] A. B. P. Lever, *Inorganic Electronic Spectroscopy*, 2nd ed, Elsevier, New York, **1968**.
[51] S. B. Jagtap, R. C. Chikate, O. S. Yemul, R. S. Ghadage, B. A. Kulkami, *J. Therm. Anal. Calorim.* **2004**, *78*, 251.
[52] C. R. Vinodkumar, M. K. Muraleedharan Nair, P. K. Radhakrishnan, *J. Therm. Anal. Calorim.* **2000**, *61*, 143.
[53] T. Hatakeyama, F. X. Quinn, *Thermal Analysis: Fundamentals and Applications to Polymer Science*, 2nd ed, John Wiley, Chichester, **1994**.
[54] S. S. Zumdahl, *Chemistry for Chemical and Biological Sciences*, University Science Books, Sausalito, CA, **2000**.
[55] F. Dimiza, S. Fountoulaki, A. N. Papadopoulos, C. A. Kontogiorgis, V. Tangoulis, C. P. Raptopoulou, V. Psycharis, A. Terzis, D. P. Kessissoglou, G. Psomas, *Dalton Trans.* **2011**, *40*, 8555.
[56] A. Sitlani, E. C. Long, A. M. Pyle, J. K. Barton, *J. Am. Chem. Soc.* **1992**, *114*, 2303.
[57] D. Mandal, M. Chauhan, F. Arjmand, G. Aromi, D. Ray, *Dalton Trans.* **2009**, 9183.
[58] M. N. Dehkordi, A. K. Bordbar, M. A. Mehrgardi, V. Mirkhani, *Spectrochim. Acta A* **2012**, *90*, 50.
[59] A. Kocak, H. Yilmaz, O. Faiz, O. Andac, *Polyhedron* **2016**, *104*, 106.
[60] C. W. Jiang, H. Chao, H. Li, L. N. Ji, *J. Inorg. Biochem.* **2009**, *93*, 247.
[61] H. Wu, J. Yuan, Y. Bai, H. Wang, G. Pan, J. Kong, *J. Photochem. Photobiol. B* **2012**, *116*, 13.
[62] F. Arjmand, S. Parveen, M. Afzal, M. Shahid, *J. Photochem. Photobiol. B* **2012**, *114*, 15.
[63] L. H. Abdel-Rahman, A. M. Abu-Dief, M. Ismael, M. A. A. Mohamed, N. A. Hashem, *J. Mol. Struct.* **2016**, *1103*, 232.
[64] L. K. Arthur, *Clin. Microbiol. Rev.* **2003**, *16*, 673.
[65] T. Arun, R. Subramanian, N. Raman, *J. Photochem. Photobiol. B* **2016**, *154*, 67.

Supporting information

Additional supporting information may be found in the online version of this article at the publisher's web-site.